# ENHANCED MULTISTATIC ACTIVE SONAR SIGNAL PROCESSING

*Kexin Zhao, Junli Liang, Johan Karlsson, and Jian Li*

Department of Electrical and Computer Engineering
University of Florida, Gainesville, FL

## ABSTRACT

This paper focuses on two signal processing aspects of multistatic active sonar systems, namely enhanced range-Doppler imaging and improved target parameter estimation. The main contributions of this paper are: i) a hybrid dense-sparse method is proposed to generate range-Doppler images with both low sidelobe levels and high accuracy; ii) a generalized K-Means clustering (GKC) method for target association is developed to associate the range measurements from different transmitter-receiver pairs; iii) the extended invariance principle-based weighted least-squares (EXIP-WLS) method is developed for accurate target position and velocity estimation. The effectiveness of the proposed multistatic active sonar system is verified using numerical examples.

***Index Terms***— Multistatic active sonar, generalized K-Means clustering method, extended invariance principle-based weighted least-squares method

## 1. INTRODUCTION

Multistatic active sonar systems involve the transmission and reception of multiple probing sequences and can achieve significantly enhanced performance of target detection and localization through exploiting spatial diversity [1–3]. In this paper, we consider two important signal processing aspects of such systems, namely range-Doppler imaging and target parameter estimation.

The receiver filter design plays a critical role in the overall performance of a multistatic active sonar system since it directly determines the quality of range-Doppler imaging and affects the accuracy of the subsequent target parameter estimation [4]. In this paper, we propose a hybrid dense-sparse range-Doppler imaging method (named IAA-MAP), which first applies the iterative adaptive approach (IAA) [5] to obtain accurate and dense range-Doppler images, and then achieve sparsity by using one step of the sparse learning via iterative minimization (SLIM) method [6]. We show that IAA-MAP can improve resolution and reduce sidelobe levels simultaneously while maintaining high accuracy.

This work was supported in part by the Office of Naval Research (ONR) under Grant No. N00014-12-1-0381.

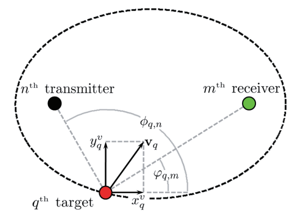


**Fig. 1**. A generic active sonar scenario for the $n$th transmitter, the $m$th receiver, and the $q$th target.

In the presence of multiple targets in the field of view, the failure in associating the peaks (after the direct blasts are removed) of the range-Doppler images could cause severe performance degradations of target parameter estimation [7]. To efficiently solve this problem, we develop a generalized K-Means clustering [8] (GKC) method for peak association to reduce the intensive computational burden required by the brute-force association (BFA) method.

Based on the fact that different transmitter-receiver pairs have different reflection coefficients, we develop an extended invariance principle-based weighted least-squares (EXIP-WLS) method for target position and velocity estimation. More specifically, nonlinear algebraic equations are approximated as linear ones via Taylor expansion and the target position and velocity estimates are refined in an iterative manner using weighting [9].

The prior work in [10] focuses on range-Doppler imaging using various adaptive filtering techniques while the work presented here adopts the IAA-MAP method to provide enhanced imaging performance and also develops algorithms for the subsequent target association and parameter estimation problems when multiple targets are at field of interest.

## 2. RANGE-DOPPLER IMAGING

Consider a two-dimensional (2D) multistatic active sonar system equipped with $N$ stationary transmitters and $M$ stationary receivers and $Q$ targets are moving in the region of interest. Denote $\mathbf{t}_n = [x_n^t, y_n^t]^T$, $\mathbf{r}_m = [x_m^r, y_m^r]^T$, and $\boldsymbol{\theta}_q = [x_q^\theta, y_q^\theta]^T$ as the Cartesian coordinate vectors of the $n^{\text{th}}$ transmitter, the $m^{\text{th}}$ receiver, and the $q^{\text{th}}$ target, respectively. Further, $N$ pings $\{s_n(t)\}_{n=1}^N$ are transmitted by the $N$ transmitters respectively and simultaneously, and every receiver is assumed to have perfect knowledge of $\{s_n(t)\}_{n=1}^N$. Figure 1 shows a generic sensing scenario for the $n^{\text{th}}$ transmitter, the $m^{\text{th}}$ receiver, and the $q^{\text{th}}$ target, in which $\mathbf{v}_q = [x_q^v, y_q^v]^T$ is the velocity vector of the $q^{\text{th}}$ target in the Cartesian coordinate. Additionally, $\phi_{q,n} = \cos^{-1}\left((x_q^\theta - x_n^t)/\|\boldsymbol{\theta}_q - \mathbf{t}_n\|\right)$ and $\varphi_{q,m} = \cos^{-1}\left((x_q^\theta - x_m^r)/\|\boldsymbol{\theta}_q - \mathbf{r}_m\|\right)$ are the bearing angles measured from the east to the line connecting $\boldsymbol{\theta}_q$ and $\mathbf{t}_n$ and the line connecting $\boldsymbol{\theta}_q$ and $\mathbf{r}_m$, respectively.

In a generic sonar scenario, the reflected echo $s_{n,q,m}(t)$ and the transmitted ping $s_n(t)$ are related through:

$$s_{n,q,m}(t) = \kappa_{n,q,m} \cdot s_n\left(\alpha_{n,q,m}\left(t - \tau_{n,q,m}\right)\right), \qquad (1)$$

where $\kappa_{n,q,m}$ is the complex-valued reflection coefficient,

$$\tau_{n,q,m} = \frac{\varrho_{n,m}(\theta_q)}{c} \qquad (2)$$

is the propagation time delay determined as the ratio of the target range $\varrho_{n,m}(\theta_q) = \|\boldsymbol{\theta}_q - \mathbf{t}_n\| + \|\boldsymbol{\theta}_q - \mathbf{r}_m\|$ to the underwater speed $c$, and

$$\alpha_{n,q,m} = \frac{c + x_q^v \cos\varphi_{q,m} + y_q^v \sin\varphi_{q,m}}{c + x_q^v \cos\phi_{q,n} + y_q^v \sin\phi_{q,n}} \qquad (3)$$

is the Doppler scaling factor.

The direct blast from the $n^{\text{th}}$ transmitter to the $m^{\text{th}}$ receiver, say $s_{n,m}(t)$, can be written as $s_{n,m}(t) = \kappa_{n,m} \cdot s_n\left(t - \tau_{n,m}\right)$, which does not suffer from Doppler scaling for stationary transmitter and receiver platforms. By taking into account the contributions from all of the $N$ transmitters and $Q$ targets, the received signal $y_m(t)$ acquired at the $m^{\text{th}}$ receiver of the multistatic active sonar systems can be represented as:

$$y_m(t) = \sum_{n=1}^{N}\sum_{q=1}^{Q} s_{n,q,m}(t) + \sum_{n=1}^{N} s_{n,m}(t) + e_m(t), \qquad (4)$$

for $m = 1, \ldots, M$, where $e_m(t)$ represents the additive noise.

The time delay and Doppler regions of interest are separately divided into $R$ and $L$ points, and there are $RL$ pixels in total in a range-Doppler image. Let $\{\tau_r, \alpha_l\}$ be the time delay-Doppler pair of the potential target and $\kappa_{n,m,r,l}$ be the target reflection coefficient associated with the $\{\tau_r, \alpha_l\}$ pair and with respect to the $n^{\text{th}}$ transmitter and the $m^{\text{th}}$ receiver. Thus the received signal $y_m(t)$ acquired at the $m^{\text{th}}$ receiver can be rewritten as

$$y_m(t) = \sum_{n=1}^{N}\sum_{r=1}^{R}\sum_{l=1}^{L} s_{n,m,r,l}(t) + e_m(t), \qquad (5)$$

where $s_{n,m,r,l}(t) = \kappa_{n,m,r,l} \cdot s_n(\alpha_l(t - \tau_r))$ is the reflected echo corresponding to the $n^{\text{th}}$ transmitted ping $s_n(t)$ and the $\{\tau_r, \alpha_l\}$ pair. The vector form of (5), $\mathbf{y}_m = \mathbf{S}_m \boldsymbol{\kappa}_m + \mathbf{e}_m$, describes a standard sparse representation problem, i.e., to estimate the sparse vector $\boldsymbol{\kappa}_m$ given the measurement vector $\mathbf{y}_m$ and the dictionary $\mathbf{S}_m$.

To obtain $\boldsymbol{\kappa}_m$ and form the range-Doppler images of size $R \times L$, we adopt the IAA-MAP method, which firstly applies the iterative adaptive approach (IAA) to obtain accurate and dense range-Doppler images and then achieves sparsity by using one step of SLIM-0 [6]. Due to the accurate and robust IAA result and a single step of SLIM-0, IAA-MAP is robust, sparse and accurate. The merits of IAA-MAP are desirable for achieving improved target parameter estimation.

## 3. TARGET PARAMETER ESTIMATION

In this section, the GKC method is introduced to associate these orderless range estimates with the corresponding targets and the EXIP-WLS method is presented to estimate the target positions and velocities.

### 3.1. Peak (Range) Association Using GKC

Given the range-Doppler images, we use the Bayesian information criterion (BIC) [11], to estimate the target number $Q$ and locate the corresponding peaks to determine ranges and Dopplers. When there are multiple targets in the field of interest, i.e., $Q \geq 2$, we need to solve the target association problem, which aims to determine a proper one-to-one correspondence between the $Q$ targets and the $Q$ peaks of each range-Doppler image.

To solve this association problem, let $\{\rho_{n,q,m}\}$ denote a collection of target range estimates obtained from the range-Doppler images and we develop a generalized K-Means [8] clustering (GKC) method by minimizing

$$\sum_{i=1}^{Q}\sum_{q=1}^{Q}\sum_{n=1}^{N}\sum_{m=1}^{M} \delta(i,q,n,m)|\rho_{n,q,m} - \|\boldsymbol{\theta}_i - \mathbf{t}_n\| - \|\boldsymbol{\theta}_i - \mathbf{r}_m\||, \qquad (6)$$

where $\delta(i,q,n,m) = 1$ if and only if $\rho_{n,q,m}$ is classified into the $i$th class; otherwise, $\delta(i,q,n,m) = 0$. This cost function implies that it is actually a combined optimization problem of the peak association and target position estimation. For ease of exposition, the outline of the proposed GKC method, which omits the details of target position estimation, is as follows:

1. *Initialization*: Randomly assign $Q$ ranges estimates (peaks) of each image with labels $1, 2, ..., Q$;
2. *Update of "Means"*:
   For $i = 1$ to $Q$
   From the $NM$ range estimates with current label $i$, we determine the $i^{\text{th}}$ target position denoted as $\hat{\boldsymbol{\theta}}_i$;
   Plugging $\hat{\boldsymbol{\theta}}_i$ into $\|\boldsymbol{\theta}_i - \mathbf{t}_n\| + \|\boldsymbol{\theta}_i - \mathbf{r}_m\|$ yields the new "means" $\|\hat{\boldsymbol{\theta}}_i - \mathbf{t}_n\| + \|\hat{\boldsymbol{\theta}}_i - \mathbf{r}_m\|$ for $\{n, m\}$.

3. *Re-assignment of Labels*:
For $n = 1, \ldots, N$, $m = 1, \ldots, M$, and $q = 1, \ldots, Q$
Assign the range estimate $\rho_{n,q,m}$ to the $i^{\text{th}}$ class (Label $i$) if and only if

$$\left|\rho_{n,q,m} - \left(\|\hat{\boldsymbol{\theta}}_i - \mathbf{t}_n\| + \|\hat{\boldsymbol{\theta}}_i - \mathbf{r}_m\|\right)\right| = \min_{p\in(1,2,\ldots,Q)} \left|\rho_{n,q,m} - \left(\|\hat{\boldsymbol{\theta}}_p - \mathbf{t}_n\| + \|\hat{\boldsymbol{\theta}}_p - \mathbf{r}_m\|\right)\right|.$$

4. *Repeat Steps 2) and 3) until convergence*.

The proposed GKC approach is more efficient than the brute-force association (BFA) method because the latter considers all possible associations while the former initializes with one random candidate and converge to the correct association pattern after a few iterations.

### 3.2. Target Position and Velocity Estimation Using EXIP-WLS

*Theorem 1* [12]: Assume that a one-to-one function $f$ exists and satisfies $\boldsymbol{\xi} = f(\boldsymbol{\theta}) \in D_{\boldsymbol{\xi}}, \forall \boldsymbol{\theta} \in D_{\boldsymbol{\theta}}$. If $\lim_{\mathcal{L}\to\infty} \hat{\boldsymbol{\xi}} = \lim_{\mathcal{L}\to\infty} f(\hat{\boldsymbol{\theta}})$, then

$$\hat{\hat{\boldsymbol{\theta}}} = \arg\min_{\boldsymbol{\theta}} \left[\hat{\boldsymbol{\xi}} - f(\boldsymbol{\theta})\right]^T \mathbf{W} \left[\hat{\boldsymbol{\xi}} - f(\boldsymbol{\theta})\right] \tag{7}$$

is asymptotically (when the number of data samples $\mathcal{L}$ is large) equivalent to the estimate $\hat{\boldsymbol{\theta}}$, with the weighting matrix $\mathbf{W} = E\left[\frac{\partial^2 ln(\mathbf{Y})}{\partial\boldsymbol{\xi}\partial\boldsymbol{\xi}^T}\right]\Big|_{\boldsymbol{\xi}=\hat{\boldsymbol{\xi}}}$, which is obtained from the corresponding block of Fisher Information matrix (FIM) that is related to the signal parameter vector $\boldsymbol{\xi}$ of the unstructured model. The related proof can be found in [12].

In this subsection, we firstly apply EXIP to estimate $\boldsymbol{\theta}_q$ from the $NM$ range estimates $\rho_{n,q,m}(\boldsymbol{\theta}_q)$ with Label $q$.

Define

$$\boldsymbol{\xi}_1 = \left[\rho_{1,q,1} \ldots \rho_{N,q,1} \quad \rho_{1,q,2} \ldots \rho_{N,q,M}\right]^T \tag{8}$$

and

$$f_1(\boldsymbol{\theta}_q) = \left[\varrho_{1,1}(\boldsymbol{\theta}_q) \ldots \varrho_{N,1}(\boldsymbol{\theta}_q) \quad \varrho_{1,2}(\boldsymbol{\theta}_q) \ldots \varrho_{N,M}(\boldsymbol{\theta}_q)\right]^T, \tag{9}$$

then we can apply (7) to obtain an estimate of $\boldsymbol{\theta}_q$ that is asymptotically equivalent to the maximum likelihood estimate of the structured model. However, $f_1(\boldsymbol{\theta}_q)$ is a nonlinear function of $\boldsymbol{\theta}_q$ and thus a search over a 2D space is required. To avoid such a computationally intensive search, we develop an EXIP-based iterative and weighted least square (EXIP-WLS) method for target position estimation, in which these nonlinear equations are approximated only by the linear parts of their Taylor expansion to refine the target position estimate in an iterative manner.

Given an initial guess of the target location, denoted as $\hat{\boldsymbol{\theta}}_q = [\hat{x}_q \quad \hat{y}_q]^T$ , and the error $\boldsymbol{\Delta}_q^\theta$ between the true target position $\boldsymbol{\theta}_q$ and the estimate $\hat{\boldsymbol{\theta}}_q$ can be given by $\boldsymbol{\Delta}_q^\theta = \boldsymbol{\theta}_q - \hat{\boldsymbol{\theta}}_q$. Thus, the true target range $\varrho_{n,m}(\boldsymbol{\theta}_q)$ can be approximated by the linear part of its Taylor expansion: $\varrho_{n,m}(\boldsymbol{\theta}_q) \approx \varrho_{n,m}(\hat{\boldsymbol{\theta}}_q) + \left(\boldsymbol{\Delta}_q^\theta\right)^T \nabla\varrho_{n,m}(\hat{\boldsymbol{\theta}}_q)$, where $\nabla(\cdot)$ denotes the gradient vector, and $\nabla\varrho_{n,m}(\hat{\boldsymbol{\theta}}_q) = \left[\cos\hat{\phi}_{q,n} + \cos\hat{\varphi}_{q,m},\ \sin\hat{\phi}_{q,n} + \sin\hat{\varphi}_{q,m}\right]^T$.

Define

$$\mathbf{D}_1 = \left[\nabla\varrho_{1,1}(\boldsymbol{\theta}_q) \ldots \nabla\varrho_{N,1}(\boldsymbol{\theta}_q)\, \nabla\varrho_{1,2}(\boldsymbol{\theta}_q) \ldots \nabla\varrho_{N,M}(\boldsymbol{\theta}_q)\right]^T, \tag{10}$$

and

$$\mathbf{a}_1 = \boldsymbol{\xi}_1 - f_1(\hat{\boldsymbol{\theta}}_q), \tag{11}$$

then (7) can be approximately transformed into the following problem:

$$\hat{\boldsymbol{\Delta}}_q^\theta = \arg\min_{\boldsymbol{\Delta}_q^\theta} \left[\mathbf{a}_1 - \mathbf{D}_1\boldsymbol{\Delta}_q^\theta\right]^T \mathbf{W}_1 \left[\mathbf{a}_1 - \mathbf{D}_1\boldsymbol{\Delta}_q^\theta\right], \tag{12}$$

where $\mathbf{W}_1$ is the block matrix of FIM that is related to the signal parameter vector $\boldsymbol{\xi}_1$, and its solution is given by $\hat{\boldsymbol{\Delta}}_q^\theta = \left(\mathbf{D}_1^T\mathbf{W}_1\mathbf{D}_1\right)^{-1}\mathbf{D}_1^T\mathbf{W}_1\mathbf{a}_1$. Once $\hat{\boldsymbol{\Delta}}_q^\theta$ is available, the target position estimate is updated as $\hat{\boldsymbol{\theta}}_q + \hat{\boldsymbol{\Delta}}_q^\theta$. To refine the estimate, we repeat the above procedure until convergence (e.g., when $\|\hat{\boldsymbol{\Delta}}_q^\theta\|$ becomes essentially zero).

We remark that when $\mathbf{W}_1 = \mathbf{I}$, the EXIP-WLS-based target position estimation approach degrades into an Unweighted Least Square (ULS) one, which treats all range measurements equally. However, in practice different transmitter-receiver pairs encounter different reflection coefficients. The EXIP-based weighting scheme exploits the fact that not all transmitter-receiver pairs are created equally for a particular target and thus should improve the accuracy of the target position estimation.

Next we consider applying EXIP to estimate $\mathbf{v}_q$ from the $NM$ Doppler estimates $\alpha_{n,q,m}$ obtained from the range-Doppler imaging results. Similarly, define

$$\boldsymbol{\xi}_2 = \left[\alpha_{1,q,1} \ldots \alpha_{N,q,1} \quad \alpha_{1,q,2} \ldots \alpha_{N,q,M}\right]^T \tag{13}$$

as the related parameter vector of the unstructured model, and

$$f_2(\mathbf{v}_q) = \left[\psi_{1,1}(\mathbf{v}_q) \ldots \psi_{N,1}(\mathbf{v}_q)\, \psi_{1,2}(\mathbf{v}_q) \ldots \psi_{N,M}(\mathbf{v}_q)\right]^T \tag{14}$$

is a one-to-one function of $\mathbf{v}_q$ in the unstructured model, where $\psi_{n,m}(\mathbf{v}_q) = \frac{c + x_q^v \cos\varphi_{q,m} + y_q^v \sin\varphi_{q,m}}{c + x_q^v \cos\phi_{q,n} + y_q^v \sin\phi_{q,n}}$. Thus, we can construct an object function similar to (7):

$$\hat{\mathbf{v}}_q = \arg\min_{\mathbf{v}_q} \left[\boldsymbol{\xi}_2 - f_2(\mathbf{v}_q)\right]^T \mathbf{W}_2 \left[\boldsymbol{\xi}_2 - f_2(\mathbf{v}_q)\right], \tag{15}$$

where $\mathbf{W}_2$ is the block matrix of FIM that is related to the signal parameter vector $\boldsymbol{\xi}_2$. $f_2(\mathbf{v}_q)$ is the nonlinear function of

**Table 1**. The noise power and the norm of the simulated amplitude and phase modifications.

| With respect to Rx1 | | | | |
|---|---|---|---|---|
| $\lvert\kappa_{1,1,1}\rvert$ | $\lvert\kappa_{1,2,1}\rvert$ | $\lvert\kappa_{2,1,1}\rvert$ | $\lvert\kappa_{2,2,1}\rvert$ | $\eta_1$ |
| 0.08 | 0.2 | 0.2 | 0.3 | $-10$ dB |
| **With respect to Rx2** | | | | |
| $\lvert\kappa_{1,1,2}\rvert$ | $\lvert\kappa_{1,2,2}\rvert$ | $\lvert\kappa_{2,1,2}\rvert$ | $\lvert\kappa_{2,2,2}\rvert$ | $\eta_2$ |
| 0.24 | 0.1 | 0.16 | 0.3 | $-10$ dB |

**Table 2**. RMSE of Parameter Estimates Using ULS and EXIP-WLS.

| Method | Target 1 | | Target 2 | |
|---|---|---|---|---|
| | $\hat{\boldsymbol{\theta}}_1$(dB) | $\hat{\mathbf{v}}_1$(dB) | $\hat{\boldsymbol{\theta}}_2$(dB) | $\hat{\mathbf{v}}_2$(dB) |
| ULS | -9.8561 | -19.7429 | -5.7636 | -15.6197 |
| EXIP-WLS | -13.6826 | -22.3587 | -8.8532 | -18.1237 |

$\mathbf{v}_q$ and thus similar Taylor approximation and iterative WLS can be applied to determine the target velocity $\mathbf{v}_q$. Since the Doppler and range measurements are paired, the velocity and position estimates are paired naturally.

## 4. SIMULATION RESULTS

Consider a multistatic active sonar system equipped with $N = 2$ transmitters and $M = 2$ receivers. The coordinate vectors of the two receivers Rx1 and Rx2 are $\mathbf{r}_1 = [2000, 0]^T$ and $\mathbf{r}_2 = [0, 2000]^T$, respectively (in unit of meter). Two transmitters, Tx1 and Tx2, are located at $\mathbf{t}_1 = [0, 0]^T$ and $\mathbf{t}_2 = [2000, 2000]^T$, respectively, and transmit two random phase (RP) sequences simultaneously. The RP sequences are unimodular with phases independently and uniformly distributed over $[0, 2\pi)$. There are $Q = 2$ targets moving in the filed of view. The first target, located at $\boldsymbol{\theta}_1 = [1000, 995]^T$, is moving at a velocity of $\mathbf{v}_1 = [\frac{-1.8}{\sqrt{2}}, \frac{-1.8}{\sqrt{2}}]^T$ knots. The second target is located at $\boldsymbol{\theta}_2 = [1050, 965]^T$ and is moving at $\mathbf{v}_2 = [0, -2]^T$ knots. The Doppler bins correspond to Doppler scaling factors ranging from 0.9976 to 1.0024. The zero-mean white Gaussian noise with a power of $\eta_1$ or $\eta_2$ is added to the measurements acquired at Rx1 or Rx2, respectively. The noise power and the norm of the target reflection coefficients are listed in Table 1.

The range-Doppler images produced by the matched filter (MF), IAA, SLIM-1, and IAA-MAP are shown in Figures 2(a)-2(d), respectively (for space reason, only one transmitter-receiver pair is given; in addition, the direct blast is removed due to available predictable locations). The intensity of all range-Doppler images is normalized so that the peak is at 0 dB and is clipped at $-40$ dB. We can see that unlike the MF images which is mired with background noise and difficult to detect the two targets, IAA, SLIM-1, and IAA-MAP all possess excellent interference suppression capabilities and produce much sharper images. Specifically, IAA-MAP provides

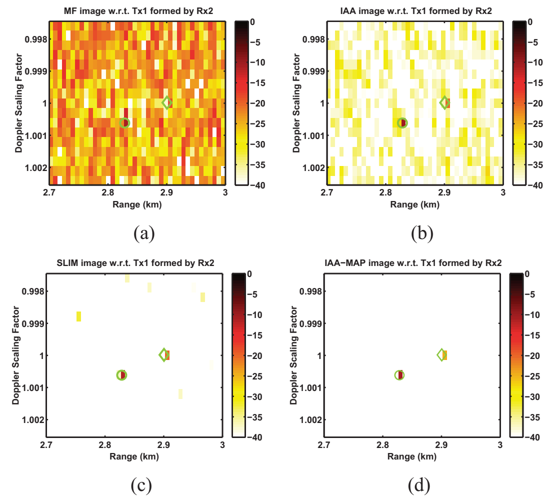


**Fig. 2**. Range-Doppler images produced by a multistatic active sonar system using various receiver filters.

more accurate estimates than SLIM-1, while maintaining a significantly lower sidelobe level than IAA. IAA-MAP provides the cleanest range-Doppler images among all methods considered herein.

From the two peaks of each range-Doppler image given by IAA-MAP, we obtain four pairs of range measurements (in unit of kilometer), i.e.,$\{2.7825, 2.8200\}$, $\{2.7600, 2.8275\}$, $\{2.8275, 2.9025\}$, and $\{2.8350, 2.8800\}$. For this multistatic active sonar system equipped with 2 transmitters and 2 receivers, there are 8 possible associations for the case of 2 targets. BFA needs to consider all possibilities, and obtains the correct association pattern at the cost of 1.23 seconds on an ordinary workstation (Intel Xeon E5506 processor 2.13G Hz, 12GB RAM, Windows 7 64-bit, and MATLAB R2010b). In comparison, the proposed GKC method only requires 0.56 seconds due to its efficient search. Finally, two groups of associated range measurements are obtained as: $\{2.7825, 2.7600, 2.9025, 2.8800\}$ and $\{2.8200, 2.8275, 2.8275, 2.8350\}$. The root mean-squared error (RMSE) of the estimated target positions and velocities obtained via the EXIP-WLS and ULS methods from 100 Monte Carlo trials are listed in Table 2, from which we can see that the EXIP-based weighting scheme significantly improves the estimation accuracy.

## 5. CONCLUSIONS

We have considered range-Doppler imaging using IAA-MAP and target parameter estimation using GKC and EXIP-WLS. We have provided numerical examples to demonstrate the effectiveness of using the proposed approaches to achieve enhanced multistatic active sonar performance.

## 6. REFERENCES


[1] M. Swift, J. Riley, S. Lourey, and L. Booth, "An overview of the multistatic sonar program in Australia," *Proc. Int. Symp. on Signal Processing and its Applications,* Brisbane, Australia, pp. 321–324, August 1999.

[2] H. Cox, "Fundamentals of bistatic active sonar," *Proc. NATO Advanced Study Inst. Underwater Acoustic Data Process.*, 1989.

[3] William C. Knight, Roger G. Pridham, and Steven M. Kay, "Digital signal processing for sonar," *Proceedings of the IEEE*, vol. 69, no. 11, pp. 1451–1507, November 1981.

[4] Nadav Levanon and Eli Mozeson, *Radar Signals*, John Wiley & Sons, Inc., NY, 2004.

[5] T. Yardibi, J. Li, P. Stoica, M. Xue, and A. B. Baggeroer, "Source localization and sensing: A nonparametric iterative adaptive approach based on weighted least squares," *IEEE Transactions on Aerospace and Electronic Systems*, vol. 46, no. 1, pp. 425 – 443, Jan. 2010.

[6] X. Tan, W. Roberts, J. Li, and P. Stoica, "Sparse learning via iterative minimization with application to MIMO radar imaging," *IEEE Transactions on Signal Processing*, pp. 1088–1101, March 2011.

[7] K. R. Pattipati, S. Deb, Y. Bar-Shalom, and R. B. Jr. Washburn, "A new relaxation algorithm and passive sensor data association," *IEEE Transactions on Automatic Control*, vol. 37, no. 2, pp. 198–213, February 1992.

[8] S. P. Lloyd, "Least squares quantization in PCM," *IEEE Transactions on Information Theory*, vol. 28, no. 2, pp. 129–137, March 1982.

[9] E. D. Kaplan and C. J. Hegarty, *Understanding GPS: principles and applications*, Artech House Mobile Communications, Norwood, MA, 2006.

[10] J. Ling, J. Li, P. Stoica, and M. Datum, "Probing waveforms and adaptive receivers for active sonar," *Journal of the Acoustical Society of America*, vol. 129, no. 6, pp. 3640 – 3651, June 2011.

[11] G. Schwarz, "Estimating the dimension of a model," *The Annals of Statistics*, vol. 6, pp. 461–464, May 1978.

[12] A. Lee Swindlehurst and Petre Stoica, "Maximum likelihood methods in radar array signal processing," *Proceedings of the IEEE*, vol. 86, pp. 421–441, February 1998.